THE UNIVERSITY *of* EDINBURGH

Edinburgh Research Explorer

Alzheimer's Disease and Small Vessel Disease Differentially Affect White Matter Microstructure

OPEN ACCESS

Check for updates

RESEARCH ARTICLE

Alzheimer's Disease and Small Vessel Disease Differentially Affect White Matter Microstructure

Mario Tranfa[1,2,*] ![ORCID], Luigi Lorenzini[2,3,*], Lyduine E. Collij[2,3,4], David Vállez García[2,3], Silvia Ingala[2,3,5,6], Giuseppe Pontillo[2], Leonard Pieperhoff[2,3], Alessio Maranzano[7] ![ORCID], Robin Wolz[8], Sven Haller[9,10,11], Kaj Blennow[12,13], Giovanni Frisoni[14,15], Carole H. Sudre[12,16,17,18], Gael Chételat[19] ![ORCID], Michael Ewers[20] ![ORCID], Pierre Payoux[21,22], Adam Waldman[23,24], Pablo Martinez-Lage[25] ![ORCID], Adam J. Schwarz[26,27], Craig W. Ritchie[28,29], Joanna M. Wardlaw[23,30] ![ORCID], Juan Domingo Gispert[31,32,33,34], Arturo Brunetti[1], Henk J. M. M. Mutsaerts[3,35] ![ORCID], Alle Meije Wink[2,3] & Frederik Barkhof[2,36]

[1]Department of Advanced Biomedical Sciences, University "Federico II", Naples, Italy
[2]Department of Radiology and Nuclear Medicine, Amsterdam University Medical Centre, Vrije Universiteit, Amsterdam, The Netherlands
[3]Amsterdam Neuroscience, Brain Imaging, Amsterdam, The Netherlands
[4]Clinical Memory Research Unit, Department of Clinical Sciences, Lund University, Malmö, Sweden
[5]Department of Radiology, Copenhagen University Hospital Rigshospitalet, Copenhagen, Denmark
[6]Cerebriu A/S, Copenhagen, Denmark
[7]Department of Neurology and Laboratory of Neuroscience, IRCCS Istituto Auxologico Italiano, Milan, Italy
[8]IXICO, London, UK
[9]CIMC - Centre d'Imagerie Médicale de Cornavin, Geneva, Switzerland
[10]Department of Surgical Sciences, Radiology, Uppsala University, Uppsala, Sweden
[11]Department of Radiology, Beijing Tiantan Hospital, Capital Medical University, Beijing, China
[12]Department of Psychiatry and Neurochemistry, Institute of Neuroscience and Physiology, The Sahlgrenska Academy at the University of Gothenburg, Gothenburg, Sweden
[13]Clinical Neurochemistry Laboratory, Sahlgrenska University Hospital, Mölndal, Sweden
[14]Laboratory Alzheimer's Neuroimaging & Epidemiology, IRCCS Istituto Centro San Giovanni di Dio Fatebenefratelli, Brescia, Italy
[15]University Hospitals and University of Geneva, Geneva, Switzerland
[16]Department of Medical Physics and Biomedical Engineering, Centre for Medical Image Computing (CMIC), University College London (UCL), London, UK
[17]MRC Unit for Lifelong Health & Ageing at UCL, University College London, London, UK
[18]School of Biomedical Engineering and Imaging Sciences, King's College London, London, UK
[19]Normandie Univ, Unicaen, Inserm, U1237, PhIND "Physiopathology and Imaging of Neurological Disorders", institut Blood-and-Brain @ Caen-Normandie, Cyceron, Université de Normandie, Caen, France
[20]German Center for Neurodegenerative Diseases (DZNE), Munich, Germany
[21]Department of Nuclear Medicine, Toulouse University Hospital, Toulouse, France
[22]ToNIC, Toulouse NeuroImaging Center, University of Toulouse, Inserm, UPS, Toulouse, France
[23]Centre for Clinical Brain Sciences, The University of Edinburgh, Edinburgh, UK
[24]Department of Medicine, Imperial College London, London, UK
[25]Centro de Investigación y Terapias Avanzadas, Neurología, CITA-Alzheimer Foundation, San Sebastián, Spain
[26]Takeda Pharmaceuticals, Ltd., Cambridge, Massachusetts, USA
[27]Department of Radiology and Imaging Sciences, Indiana University School of Medicine, Indianapolis, Indiana, USA
[28]Edinburgh Dementia Prevention, Centre for Clinical Brain Sciences, Outpatient Department 2, Western General Hospital, University of Edinburgh, Edinburgh, UK
[29]Brain Health Scotland, Edinburgh, UK
[30]UK Dementia Research Institute Centre at the University of Edinburgh, Edinburgh, UK
[31]Barcelonaβeta Brain Research Center (BBRC), Pasqual Maragall Foundation, Barcelona, Spain
[32]CIBER Bioingeniería, Biomateriales y Nanomedicina (CIBER-BBN), Madrid, Spain
[33]IMIM (Hospital del Mar Medical Research Institute), Barcelona, Spain
[34]Universitat Pompeu Fabra, Barcelona, Spain
[35]Ghent Institute for Functional and Metabolic Imaging (GIfMI), Ghent University, Ghent, Belgium
[36]Institute of Neurology and Healthcare Engineering, University College London, London, UK

Correspondence
Mario Tranfa, Department of Advanced Biomedical Sciences, University "Federico II", Via Pansini 5, Naples 80131, Italy.

Abstract

Objective: Alzheimer's disease (AD) and cerebral small vessel disease (cSVD), the two most common causes of dementia, are characterized by white matter

Tel: +390817462560. Fax: +390817463527.
E-mail: m.tranfa@amsterdamumc.nl

*These authors contributed equally to the
study.

(WM) alterations diverging from the physiological changes occurring in healthy aging. Diffusion tensor imaging (DTI) is a valuable tool to quantify WM integrity non-invasively and identify the determinants of such alterations. Here, we investigated main effects and interactions of AD pathology, APOE-ε4, cSVD, and cardiovascular risk on spatial patterns of WM alterations in non-demented older adults. **Methods**: Within the prospective European Prevention of Alzheimer's Dementia study, we selected 606 participants (64.9 ± 7.2 years, 376 females) with baseline cerebrospinal fluid samples of amyloid $\beta_{1\text{-}42}$ and p-Tau$_{181}$ and MRI scans, including DTI scans. Longitudinal scans (mean follow-up time = 1.3 ± 0.5 years) were obtained in a subset ($n = 223$). WM integrity was assessed by extracting fractional anisotropy and mean diffusivity in relevant tracts. To identify the determinants of WM disruption, we performed a multimodel inference to identify the best linear mixed-effects model for each tract. **Results**: AD pathology, APOE-ε4, cSVD burden, and cardiovascular risk were all associated with WM integrity within several tracts. While limbic tracts were mainly impacted by AD pathology and APOE-ε4, commissural, associative, and projection tract integrity was more related to cSVD burden and cardiovascular risk. AD pathology and cSVD did not show any significant interaction effect. **Interpretation**: Our results suggest that AD pathology and cSVD exert independent and spatially different effects on WM microstructure, supporting the role of DTI in disease monitoring and suggesting independent targets for preventive medicine approaches.

Introduction

While physiological changes in white matter (WM) microstructural integrity can be observed in healthy aging, neurodegeneration due to Alzheimer's disease (AD)[1] and cerebral small vessel disease (cSVD)[2] are characterized by accelerated myelin disruption and axonal damage and loss. Both AD and cSVD affect oligodendrocyte function, acting through iron overload, oxidative stress, and endothelial dysfunction pathways, ultimately resulting in demyelination and axonal loss.[3,4] Previous studies have investigated the interplay between AD and cSVD on white matter microstructural integrity, observing variable degrees of association when looking at different imaging biomarkers of cSVD, such as white matter hyperintensities (WMHs),[5] and cerebral microbleeds (CMBs).[6] Conflicting evidence has emerged regarding their possible interactive effects on neurodegeneration and white matter disruption, with studies supporting both a synergistic effect[7] and the independence[8] of AD from cSVD and cardiovascular risk factors. Therefore, it is still unclear whether these associations are related to shared risk factors or to the mechanistic interplay between the underlying pathological alterations.

Diffusion tensor imaging (DTI) is an MRI technique sensitive to white matter (WM) microstructural changes.[9] By measuring the diffusion properties of water molecules, it is possible to assess metrics of WM integrity such as fractional anisotropy (FA – the fraction of diffusion along one preferential direction) and mean diffusivity (MD – the average of diffusion along three main axes).[10] Decrease in FA and increase in MD have been observed from the early stages of neurodegeneration due to both AD[1] and cSVD,[2] highlighting the potential of DTI metrics as early and non-invasive imaging biomarkers. Previous studies suggest that the susceptibility to WM alterations could present disease-specific spatial patterns. In particular, while the amyloid-β (Aβ) pathological cascade of events has mostly been associated with reduction of temporal and parietal WM integrity,[11] cSVD typically relates to alterations at the level of the genu of corpus callosum (CC),[12] suggesting that these diseases could exert differential regional effects. However, although it has been shown that these pathologies often coexist,[3] whether and to what extent they interact with each other in determining WM microstructural disruption remains unclear.

The development of new targeted therapies for AD and cSVD[13,14] highlights the need for identifying the determinants of WM alterations and disentangling their individual contributions.[15] In recent years, intervention studies have been progressively focusing on the preclinical and prodromal stages of dementia, using mixed strategies to target the risk factors associated with AD[13] and cSVD.[16] As new primary and secondary prevention trials are starting, we need robust and possibly noninvasive biomarkers to properly define the enrollment criteria and serve as outcome measures of treatment efficacy in absence of cognitive decline.[13]

This study aims to explore the differential impact and possible interactions of AD pathology and cSVD, along with their associated genetic (APOE-ε4) and acquired

(cardiovascular) risk factors, on WM microstructural alterations as assessed by DTI in a large sample of non-demented older adults from the European Prevention of Alzheimer Dementia (EPAD) cohort.

Methods

Study participants

Data were drawn from the vIMI release of the EPAD cohort (www.ep-ad.org). EPAD eligibility criteria included age above 50 years and no diagnosis of dementia (Clinical Dementia Rating [CDR] scale ≤ 0.5).[17] This prospective study included 606 individuals with available cerebrospinal fluid (CSF), APOE, cerebrovascular and cardiovascular data, and MRI scans including at least T1-weighted, T2*-weighted, T2-FLAIR, and DTI sequences (voxel size = $2.0 \times 2.0 \times 2.0$ mm^3, diffusion-encoding directions = 30) (Fig. 1). Longitudinal DTI data were available for a subset of individuals ($n = 223$).

Standard protocol approvals, registrations, and patient consents

The study was approved by the ethical committees of all participating centers. All study participants provided written informed consent according to the Declaration of Helsinki.

CSF analysis and AT classification

CSF biomarkers were quantified using a harmonized pre-analytical protocol.[18] Analyses were performed with the fully automated Roche Elecsys System at the Clinical Neurochemistry Laboratory, Mölndal, Sweden.[17] Concentrations of amyloid-beta (A$\beta_{1\text{-}42}$) and phosphorylated-tau (p-Tau$_{181}$) were determined using the manufacturer's guidelines. Following previous work on the same cohort,[18] CSF A$\beta_{1\text{-}42}$ levels < 1000 pg/mL and CSF p-Tau$_{181}$ levels > 27 pg/mL were used to define amyloid positivity (A+) and tau positivity (T+), respectively. Four AT groups were derived (i.e., A-T-, A+T-, A+T+ and A-T+). A-T+ participants were excluded as they belong to the suspected non-AD pathology group.

APOE genotype

APOE genotype was determined from Taqman Genotyping of blood samples and analyzed in a single laboratory at the University of Edinburgh using QuantStudio 12KL Flex. APOE-ε4 carriers were defined as having at least one ε4 allele. Total DNA was obtained through proteinase-K digestion and alcohol precipitation of the
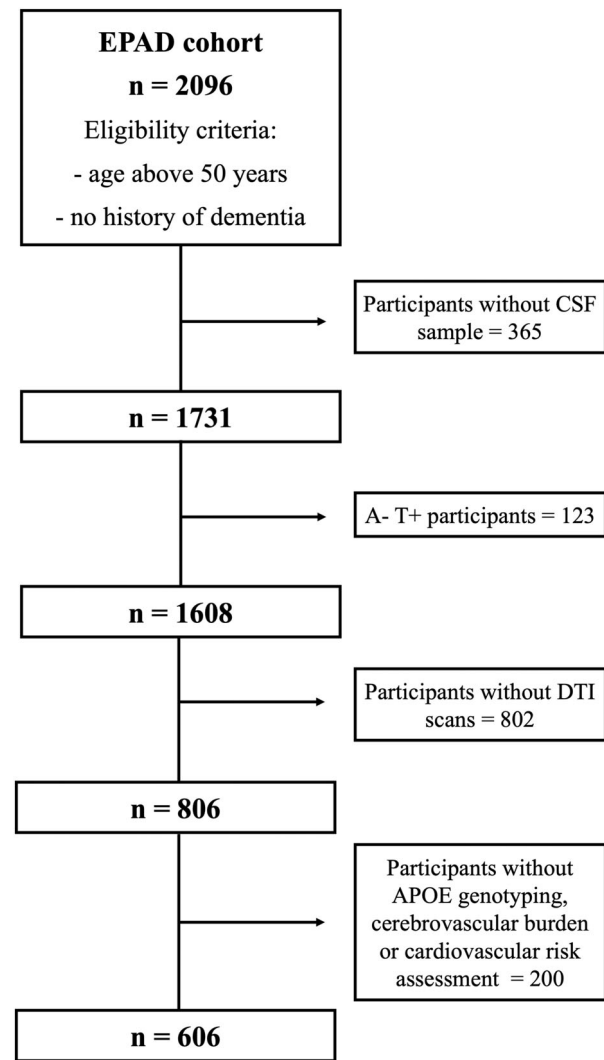
Figure 1. Flow diagram of the study. Flow diagram showing how final sample size was obtained with application of inclusion and exclusion criteria. CSF, cerebrospinal fluid; DTI, diffusion tensor imaging.

blood cellular fraction. Samples were genotyped, using the APOE-F 5′-TTGAAGGCCTA CAAATCGGAACTG-3′ and APOE-R 5′-CCGGCTGCCCAT CTCCTCCATCCG-3′ primers, for two single nucleotide polymorphisms, rs429358 and rs7412. Thus, the possible APOE alleles were determined as follows: ε1, rs429358 (C) + rs7412 (T); ε2, rs429358 (T) + rs7412 (T); ε3, rs429358 (T) + rs7412 (C); and ε4, rs429358 (C) + rs7412 (C).

Cerebrovascular factors

Visual MRI reads were centrally performed by three observers (two neuroradiologists with more than 15 years of experience; one in training) according to the STRIVE

(Standards for Reporting Vascular Changes on Neuroimaging) criteria.[19] Visual scores included a 0–4 scale for enlarged perivascular spaces (ePVS) in basal ganglia and centrum semiovale; Fazekas scale (0–3) for periventricular and deep WMHs; presence/absence of lobar CMBs, presence of more than 2 deep CMBs; and lacunes (0, 1, 2, >2). We used confirmatory factor analysis to build a cSVD-burden latent factor from the radiological indices. Subsequently, gaussian mixture modeling was applied to identify a cutoff to dichotomize the cohort in cSVD groups as cSVD+ and cSVD- (Fig. S2). More details are provided in supplementary material.

Cardiovascular risk factors (Framingham)

Individual vascular risk was computed using the Framingham Risk Score (FRS), encompassing information on age, sex, systolic blood pressure, antihypertensive medication, diabetes, smoking, total and HDL cholesterol,[20] as previously described.[21] FRS was computed with and without age correction, and uncorrected scores were used in later analysis.

MRI acquisition and processing

MRI acquisition and preprocessing details have been detailed elsewhere.[22] Briefly, diffusion-weighted images underwent geometric distortion correction using the opposed phase-encoding polarities, head motion and eddy-current correction, brain extraction, and tensor-fitting to produce FA and MD maps.

Tract-based spatial statistics

DTI maps were processed with the tract-based spatial statistics approach.[23] Brain extracted FA maps were aligned into a common space with nonlinear registration, obviating the need for an inter-session subject-specific template, as longitudinal data were not available for all participants and therefore we did not want to introduce a bias by performing an additional registration step in a subset. We created a FA skeleton mask that comprised the WM regions common to the group. Using the JHU ICBM-DTI-81 atlas,[24] FA and MD were extracted from 14 selected skeletonized tracts (Fig. 2), subdivided in commissural, associative, limbic (to distinguish them from other associative and commissural tracts, based on their involvement in AD pathophysiology)[25] and projections tracts. DTI scalars were site-harmonized using the ComBat Toolbox[26] and standardized. More details are given in supplementary material. We decided to not mask out WMHs from skeletonized tracts because we were interested in the effect of our putative determinants on the

total WM, though their impact was negligible as the percentage of WMH voxels included in the skeletonized tracts was very low on average (1.5 ± 2.9%).

Statistical analysis

Demographics were compared using chi-square and *t*-tests, as appropriate.

Variables were tested for collinearity using the *performance* R package (v. 0.10.4).

For each tract and for both scalars, we performed a multimodel inference through *MuMin* R package (v. 1.47.5) to identify the best linear mixed-effects models. Briefly, starting from a reference model containing all variables of interest, we computed all possible models based on every combination of our predictors and selected the ones having the highest second-order Akaike information criterion scores.

The reference linear mixed-effects model (computed using the *lme4* R package, v. 1.1–33) entered in the multimodel inference included a random intercept for the participant, and age and sex as covariates. The predictors included in the reference linear mixed-effects model were APOE-ε4, AT status, cSVD groups, and FRS (main effect of determinants); the time interval between MRI acquisitions (main effect of time); the pairwise interactions between APOE-ε4, AT status, cSVD groups, and FRS (interaction effect of determinants); the pairwise interactions between the time interval and APOE-ε4, AT status, cSVD groups, and FRS (main effect of determinants on longitudinal changes); the three-way interactions between the time interval and all possible pairs among APOE-ε4, AT status, cSVD groups, and FRS (interaction effect of determinants on longitudinal changes). Full formulas are given in supplementary material.

Age and sex were always included in the final models. *p*-values were adjusted for multiple testing using false discovery rate control (the Benjamini–Hochberg procedure) across the selected models and considered significant when $p_{FDR} < 0.05$.

All statistical analyses were performed using R (v. 4.2.1).

Results

Demographic and clinical data of the study participants (*n* = 606) are shown in Table 1. Mean baseline age was 64.9 ± 7.2 years, 376 participants (62.0%) were female, and 142 (23.4%) had CDR = 0.5. Mean follow-up time was 1.3 ± 0.5 years.

Participants had moderate cardiovascular risk according to FRS (mean FRS = 14.4 ± 2.3). The cSVD severity was generally low (median total Fazekas-score = 1,
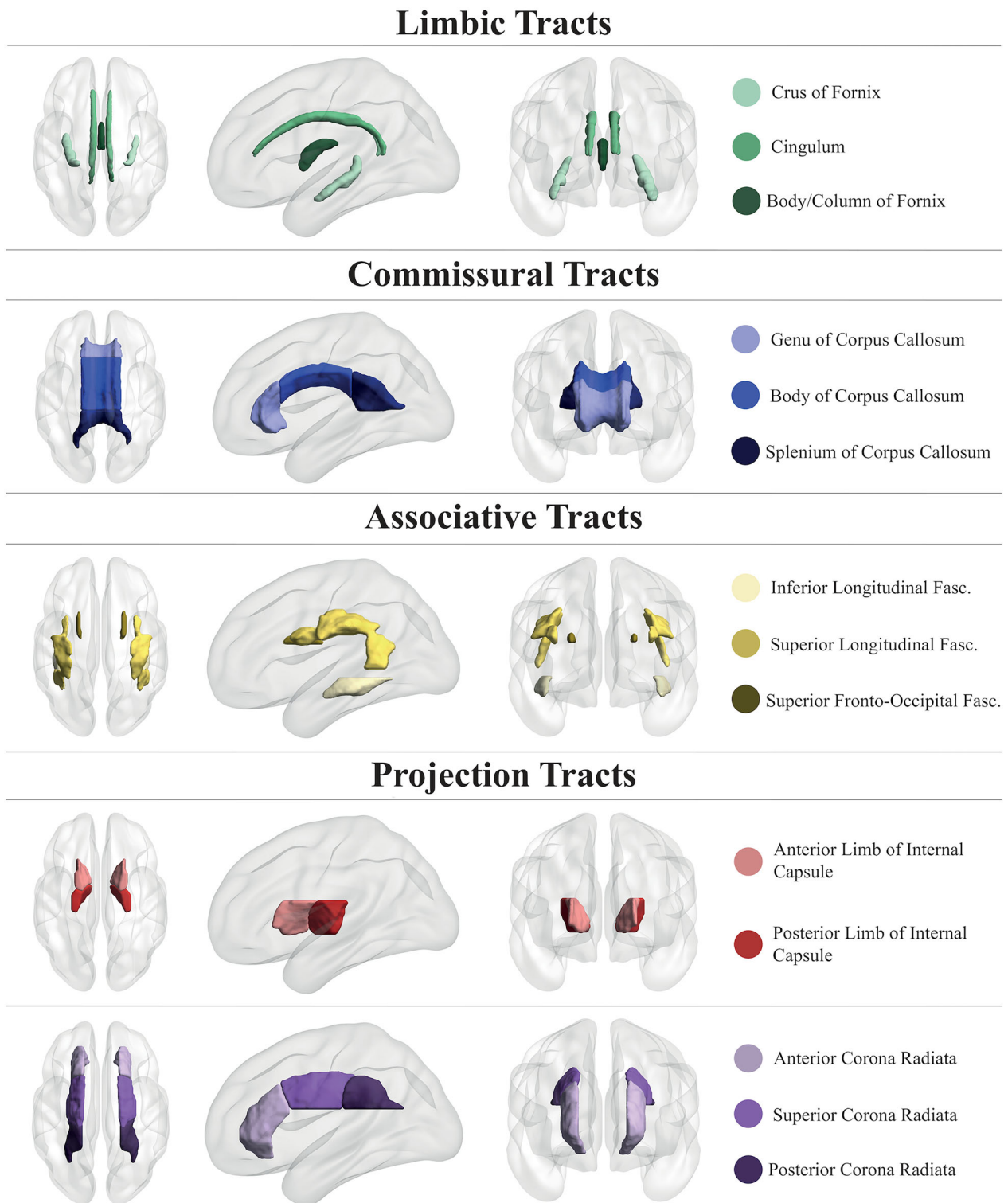
Figure 2. WM tracts selected for the study. Fasc., fasciculus; WM, white matter.

interquartile range [IQR] = 1.8). In total, 19 (3.1%) and 75 (12.4%) participants had at least two deep or one lobar CMBs, respectively. Thirty-four (5.6%) participants had at least one lacune. Median of basal ganglia and centrum semiovale ePVS was 1 for both (IQR = 0 and 1, respectively).

Effect of age and sex on WM integrity

Older age was associated with lower FA (β ranging from -0.048 to -0.015, all $p \leq 0.02$) and higher MD values (β ranging from 0.020 to 0.055, all $p \leq 0.001$) in most of the analyzed tracts. Men showed higher MD (β ranging from 0.166 to 0.367, all $p \leq 0.03$), coupled with lower FA in the column body of the fornix ($\beta = -0.343$, $p < 0.001$) and higher FA in the cingulum ($\beta = 0.266$, $p = 0.01$).

Determinants of WM integrity

Multimodel inference and linear mixed-effects models full results are shown in Tables 2, 3 and Figs. 3, 4. Predictors selected by the multimodel inference for each linear mixed-effects model are listed in Tables S1 and S2. Plots exemplifying significant longitudinal effects are reported in Fig. S2. The analysis was repeated after excluding the participants having a CDR = 0.5, and the main results were unchanged (data not shown). We decided to include those subjects in the main analysis for two main reasons. Firstly, as clinical trials are starting to move toward the preclinical stages, we wanted to simulate a real-life scenario by including all those subjects that are still non-demented and that can benefit the most from early intervention therapies. Secondly, even if by excluding those subjects we were able to confirm our main results, this comes at the cost of losing statistical power to detect meaningful biological effects, as most of the A+T+ participants belong to the CDR = 0.5 group (as shown in Table 1).

Limbic tracts

White matter integrity in limbic tracts, including cingulum, column body, and crus of the fornix, was generally associated with both AD and vascular related factors, with stronger effects dependent on the AT status.

Compared to A-T-, participants in the A+T- group had lower FA in the column body ($\beta = -0.701$, $p < 0.001$) and crus of the fornix ($\beta = -0.290$, $p = 0.03$), and higher MD in the cingulum ($\beta = 0.230$, $p = 0.01$) and column body of the fornix ($\beta = 0.546$, $p < 0.001$), while A+T+ had higher FA ($\beta = -0.300$, $p = 0.047$) and lower MD ($\beta = 0.314$, $p = 0.02$) in the cingulum. APOE-ϵ4 was associated with longitudinal decreases of FA ($\beta = -0.095$, $p = 0.006$) and increases of MD in the ($\beta = 0.107$, $p = 0.02$) in the column body of the fornix.

Moreover, cSVD+ was associated with lower baseline FA in the column body ($\beta = -0.162$, $p = 0.046$) and higher baseline ($\beta = 0.210$, $p = 0.03$) and longitudinal ($\beta = 0.178$, $p = 0.005$) MD in the crus of the fornix. FRS showed a cross-sectional effect on FA in the cingulum ($\beta = -0.049$, $p = 0.005$) in the column body of the fornix ($\beta = -0.048$, $p = 0.01$) and on MD in the crus of fornix ($\beta = 0.045$, $p = 0.01$). APOE-ϵ4 and FRS showed a significant three-way interaction with time on MD changes in the column body of the fornix ($\beta = -0.021$, $p = 0.03$).

Commissural tracts

White matter integrity in commissural tracts, including genu, body, and splenium of the CC, was mostly impacted by cerebrovascular and cardiovascular factors, most prominently in the genu of CC.

In particular, cSVD+ participants had lower baseline FA in the regions of the genu ($\beta = -0.233$, $p = 0.009$) and the splenium ($\beta = -0.267$, $p = 0.02$), and greater increases of MD over time in the genu ($\beta = 0.098$, $p = 0.03$). Higher FRS was associated with lower baseline FA in the splenium ($\beta = 0.034$, $p = 0.045$), and greater

Table 1. Demographic and clinical data of the subjects included in the study.

	Overall	A-T-	A+T-	A+T+	*p*-value
N [baseline (longitudinal)]	606 (223)	410 (143)	137 (49)	59 (31)	n.a.
Age [mean (SD)]	64.93 (7.16)	63.81 (6.99)	65.69 (6.69)	70.97 (6.12)	<0.001
Sex [m (%)]	230 (38.0)	146 (35.6)	55 (40.1)	29 (49.2)	0.11
Total follow-up time, years [mean (SD)]	1.33 (0.48)	1.36 (0.49)	1.28 (0.46)	1.30 (0.48)	0.61
CDR global score = 0.5 [*n* (%)]	142 (23.4)	71 (17.3)	36 (26.3)	35 (59.3)	<0.001
MMSE score [mean (SD)]	28.61 (1.72)	28.85 (1.46)	28.42 (2.01)	27.44 (2.10)	<0.001
APOE-ϵ4 carriers [*n* (%)]	221 (36.5)	110 (26.8)	69 (50.4)	42 (71.2)	<0.001
Framingham risk score [mean (SD)]	14.35 (4.19)	13.84 (4.19)	14.73 (3.73)	17.02 (4.14)	<0.001
cSVD+ [*n* (%)]	258 (42.6)	156 (38.0)	61 (44.5)	41 (69.5)	<0.001
Number of visits					0.07
1 visit [*n* (%)]	383 (63.2)	267 (65.1)	88 (64.2)	28 (47.4)	
2 visits [*n* (%)]	170 (28.1)	105 (25.6)	40 (29.2)	25 (42.4)	
3 visits [*n* (%)]	53 (8.7)	38 (9.3)	9 (6.6)	6 (10.2)	

CDR, clinical dementia rating; cSVD, cerebral small vessel disease; MMSE, mini mental-state examination; n.a., not applicable; SD, standard deviation.

Table 2. Different impact of individual factors on WM FA.

	Genu of CC	Body of CC	Splenium of CC	Cingulum	Column and body of the fornix	Crus of the fornix	Superior long. fasc.	Inferior long. fasc.	Superior fronto-occipital fasc.	Anterior limb of internal capsule	Posterior limb of internal capsule	Anterior corona radiata	Posterior corona radiata	Superior corona radiata
Age	**−0.015; 0.02**	**−0.022; 0.002**	−0.011; 0.14	**−0.029; <0.001**	**−0.047; <0.001**	**−0.048; <0.001**	−0.003; 0.64	**−0.017; 0.02**	−0.008; 0.31	−0.005; 0.51	0.005; 0.46	**−0.029; <0.001**	0.003; 0.65	−0.006; 0.42
Sex (m)	0.085; 0.38	−0.084; 0.38	−0.053; 0.52	**0.266; 0.01**	**−0.343; <0.001**	−0.059; 0.47	−0.102; 0.38	−0.102; 0.38	0.089; 0.38	0.161; 0.22	−0.100; 0.38	−0.060; 0.47	−0.096; 0.38	−0.107; 0.38
A+T-	/	**−0.221; 0.03**	/	−0.165; 0.09	**−0.701; <0.001**	**−0.290; 0.03**	−0.106; 0.27	**−0.292; 0.007**	−0.167; 0.08	/	**−0.225; 0.03**	**−0.284; 0.005**	**−0.240; 0.03**	−0.192; 0.06
A+T+	/	−0.117; 0.42	−0.214; 0.21	**−0.300; 0.047**	0.068; 0.75	0.210; 0.40	**−0.332; 0.04**	**−0.309; 0.047**	−0.242; 0.10	/	**−0.344; 0.04**	**−0.302; 0.04**	**−0.364; 0.03**	**−0.434; 0.02**
APOE-ε4	/	/	/	/	−0.024; 0.86	−0.027; 0.86	/	0.143; 0.21	/	/	/	/	/	/
cSVD	**−0.233; 0.009**	−0.132; 0.36	**−0.267; 0.02**	/	**−0.162; 0.046**	0.107; 0.40	**−0.365; <0.001**	**−0.262; 0.004**	**−0.596; <0.0001**	**−0.607; <0.001**	−0.029; 0.07	**−0.381; <0.0001**	**−0.304; 0.001**	**−0.214; 0.02**
FRS	−0.007; 0.70	−0.006; 0.76	**0.034; 0.045**	**−0.049; 0.005**	**−0.048; 0.01**	−0.012; 0.60	/	/	**−0.048; 0.03**	−0.031; 0.05	−0.029; 0.07	**−0.054; 0.001**	/	−0.026; 0.10
APOE-ε4*A+T-	/	/	/	/	0.271; 0.12	0.387; 0.06	/	/	/	/	/	/	/	/
APOE-ε4*A+T+	/	/	/	/	−0.352; 0.18	−0.451; 0.18	/	/	/	/	/	/	/	/
APOE-ε4*FRS	/	/	/	/	0.037; 0.15	/	/	/	/	/	/	/	/	/
APOE-ε4*cSVD	/	/	0.254; 0.11	/	/	/	/	/	/	/	/	/	/	/
FRS*cSVD	/	−0.04; 0.14	/	/	/	−0.048; 0.14	/	/	0.044; 0.14	/	/	/	/	/
Time	**−0.118; 0.02**	−0.032; 0.42	−0.024; 0.79	/	−0.029; 0.49	**−0.096; 0.04**	**−0.053; 0.01**	**−0.193; <0.001**	/	0.011; 0.80	**0.066; 0.03**	**0.071; 0.01**	/	/
A+T-*time	/	/	/	/	/	0.128; 0.15	/	0.025; 0.75	/	/	/	−0.086; 0.19	/	−0.053; 0.29
A+T+*time	/	/	/	/	/	−0.104; 0.22	/	−0.181; 0.07	/	/	/	**−0.175; 0.009**	/	**−0.138; 0.01**
APOE-ε4*time	/	/	/	/	**−0.095; 0.006**	/	/	/	/	/	/	/	/	/
FRS*time	**−0.026; 0.007**	−0.01; 0.08	−0.023; 0.07	/	0.01; 0.07	/	/	/	/	/	/	/	/	/
cSVD*time	−0.081; 0.11	/	/	/	−0.047; 0.11	−0.096; 0.11	/	/	/	−0.090; 0.11	/	/	/	/

Table showing coefficients and p_{FDR}-values of the LMEs selected by the multimodal inference to test the effect of individual factors on FA values. Predictors that were not included in at least one LME are not reported. Results are expressed as "β coefficient; p_{FDR}-value". Significant results are highlighted in bold. cSVD, cerebral small vessel disease; fasc., fasciculus; FDR, false discovery rate; FRS, Framingham risk score; LMEs, linear mixed effect models; long, longitudinal; WM, white matter; "/", predictor not included in the selected model.

Table 3. Different impact of individual factors on WM MD.

	Genu of corpus callosum	Body of corpus callosum	Splenium of corpus callosum	Cingulum	Column and body of the fornix	Crus of the fornix	Superior long. fasc.	Inferior long. fasc.	Superior fronto-occipital fasc.	Anterior limb of internal capsule	Posterior limb of internal capsule	Anterior corona radiata	Posterior corona radiata	Superior corona radiata
Age	0.045; <0.001	0.051; <0.001	0.037; <0.001	0.034; <0.001	0.055; <0.001	0.027; <0.001	0.029; <0.001	0.022; <0.001	0.039; <0.001	0.042; <0.0001	0.020; 0.001	0.043; <0.001	0.038; <0.001	0.036; <0.001
Sex (m)	0.034; 0.69	0.226; 0.004	0.174; 0.03	−0.068; 0.46	0.226; 0.004	0.131; 0.14	0.222; 0.005	0.367; <0.001	0.166; 0.03	0.053; 0.53	0.164; 0.06	0.025; 0.72	0.291; <0.001	0.276; <0.001
A+T−	/	/	/	0.230; 0.01	0.546; <0.001	/	0.253; 0.004	0.208; 0.02	/	0.205; 0.02	0.391; <0.001	0.190; 0.02	0.247; 0.004	0.279; 0.001
A+T+	/	/	/	0.314; 0.02	−0.214; 0.34	/	0.510; <0.001	0.339; 0.02	/	0.353; 0.02	0.427; 0.01	0.302; 0.02	0.255; 0.04	0.307; 0.02
APOE-ε4	/	0.083; 0.54	0.238; 0.008	/	−0.032; 0.96	/	/	0.067; 0.96	0.125; 0.54	0.024; 0.96	−0.144; 0.32	/	/	/
cSVD	−0.045; 0.77	0.005; 0.97	−0.054; 0.77	0.117; 0.44	0.160; 0.05	0.210; 0.03	0.443; <0.001	0.380; <0.001	0.562; <0.001	0.480; <0.001	0.191; 0.046	0.254; 0.046	0.357; 0.006	0.496; <0.001
FRS	0.001; 0.95	0.005; 0.83	−0.029; 0.17	0.009; 0.76	0.036; 0.07	0.045; 0.01	0.031; 0.07	0.034; 0.11	0.026; 0.17	0.020; 0.40	0.050; 0.008	0.019; 0.34	0.005; 0.83	0.028; 0.07
APOE-ε4*A+T−	/	/	/	/	−0.212; 0.42	/	/	/	/	/	/	/	/	/
APOE-ε4*A+T+	/	/	/	/	0.441; 0.08	/	/	/	/	/	/	/	/	/
APOE-ε4*FRS	/	/	/	/	−0.027; 0.44	/	/	−0.025; 0.44	−0.013; 0.59	−0.037; 0.37	/	/	/	/
APOE-ε4*cSVD	/	/	/	/	/	/	/	−0.106; 0.49	/	/	/	/	/	/
FRS*cSVD	0.058; 0.04	0.067; 0.03	0.053; 0.06	0.071; 0.03	/	/	/	/	/	0.037; 0.13	/	0.042; 0.10	0.039; 0.12	/
Time	−0.148; 0.001	0.045; 0.27	0.081; 0.13	/	0.024; 0.32	−0.135; 0.004	−0.088; 0.001	−0.120; 0.02	−0.167; 0.002	−0.021; 0.50	−0.069; 0.27	−0.076; 0.01	−0.034; 0.32	−0.037; 0.24
A+T−*time	/	/	/	/	−0.050; 0.11	/	/	0.127; 0.06	/	/	/	0.082; 0.10	/	0.097; 0.06
A+T+*time	/	0.066; 0.14	/	/	0.068; 0.15	/	/	0.248; 0.002	/	/	/	0.075; 0.18	0.078; 0.18	0.078; 0.18
APOE-ε4*time	/	/	/	/	0.107; 0.02	/	/	0.176; 0.03	0.239; 0.01	/	/	/	/	/
FRS*time	0.014; 0.07	0.016; 0.07	/	/	0.001; 0.83	/	/	0.018; 0.07	0.029; 0.007	/	−0.018; 0.11	/	0.015; 0.07	/
cSVD*time	0.098; 0.03	/	0.098; 0.13	/	/	0.178; 0.005	0.098; 0.004	0.193; 0.001	0.168; 0.001	0.152; 0.002	0.095; 0.13	0.081; 0.03	0.157; 0.003	0.096; 0.01
APOE-ε4*FRS*time	/	/	/	/	/	/	/	/	/	/	/	/	/	/

Table 3 Continued.

	Genu of corpus callosum	Body of corpus callosum	Splenium of corpus callosum	Cingulum	Column and body of the fornix	Crus of the fornix	Superior long. fasc.	Inferior long. fasc.	Superior fronto-occipital fasc.	Anterior limb of internal capsule	Posterior limb of internal capsule	Anterior corona radiata	Posterior corona radiata	Superior corona radiata
APOE-ε4*cSVD*time	/	/	/	/	**−0.021; 0.03**	/	/	**−0.040; 0.03** **−0.218; 0.02**	**−0.042; 0.03**	/	/	/	/	/
FRS*cSVD*time	/	/	/	/	/	/	/	/	/	/	/	/	−0.016; 0.13	/

Table showing coefficients and p_{FDR}-values of the LMEs selected by the multimodal inference to test the effect of individual factors on MD values. Predictors that were not included in at least one LME are not reported. Results are expressed as "β coefficient; p_{FDR}-value". Significant results are highlighted in bold. p_{FDR}, p-value; cSVD, cerebral small vessel disease; fasc., fasciculus; FDR, false discovery rate; FRS, Framingham risk score; LMEs, linear mixed effect models; long., longitudinal; WM, white matter; "/", predictor not included in the selected model.

declines of FA over time in the genu of CC ($\beta = -0.026$, $p = 0.007$). The effects of AD-related factors were circumscribed to body and splenium of CC, with A+T- participants showing lower body FA ($\beta = -0.221$, $p = 0.03$) and APOE-ε4 being associated with higher splenium MD ($\beta = 0.238$, $p = 0.008$).

Associative tracts

White matter integrity in associative tracts, including superior longitudinal, inferior longitudinal, and superior fronto-occipital fasciculi, was similarly and independently impacted by both vascular and AD-related factors. However, the integrity of the superior fronto-occipital fasciculus was independent of AD pathology.

Compared to A-T-, A+T- participants at baseline had lower FA in the inferior longitudinal ($\beta = -0.292$, $p = 0.007$), and higher MD in the inferior ($\beta = 0.208$, $p = 0.02$) and superior ($\beta = -0.042$, $p = 0.03$) longitudinal fasciculi, while A+T+ participants had lower FA and higher MD in the superior (FA: $\beta = -0.332$, $p = 0.04$; MD: $\beta = 0.510$, $p < 0.001$) and inferior (FA: $\beta = -0.309$, $p = 0.047$; MD: $\beta = 0.339$, $p = 0.02$) longitudinal fasciculi, and greater increases of MD over time in the inferior longitudinal fasciculus ($\beta = 0.248$, $p = 0.002$). APOE-ε4 was only related to greater increases of MD over time in inferior longitudinal ($\beta = 0.176$, $p = 0.03$) and superior fronto-occipital fasciculi ($\beta = 0.239$, $p = 0.01$).

CSVD+ participants had lower FA, higher MD and greater longitudinal increases of MD in all investigated associative tracts (all coefficients in Tables 2 and 3). Higher FRS scores were distinctively related to lower baseline FA ($\beta = -0.048$, $p = 0.03$) and greater decreases of MD over time in the superior fronto-occipital fasciculus ($\beta = 0.029$, $p = 0.007$).

Even if some significant three-way effects on MD changes were retained for inferior longitudinal (APOE-ε4*FRS*time with $\beta = -0.040$ and $p = 0.03$, and APOE-ε4*cSVD+*time with $\beta = -0.218$ and $p = 0.02$) and superior fronto-occipital fasciculi (FRS*APOE-ε4*time with $\beta = -0.042$ and $p = 0.03$), none of them included interactions between AD pathology and cerebrovascular factors.

Projection tracts

Projection tracts included anterior and posterior limbs of internal capsule, and anterior, posterior, and superior corona radiata. While the corona radiata was comparably impacted by AD and cSVD, integrity of the anterior and posterior limbs of the internal capsule was mostly linked to cSVD and AD-related factors, respectively.

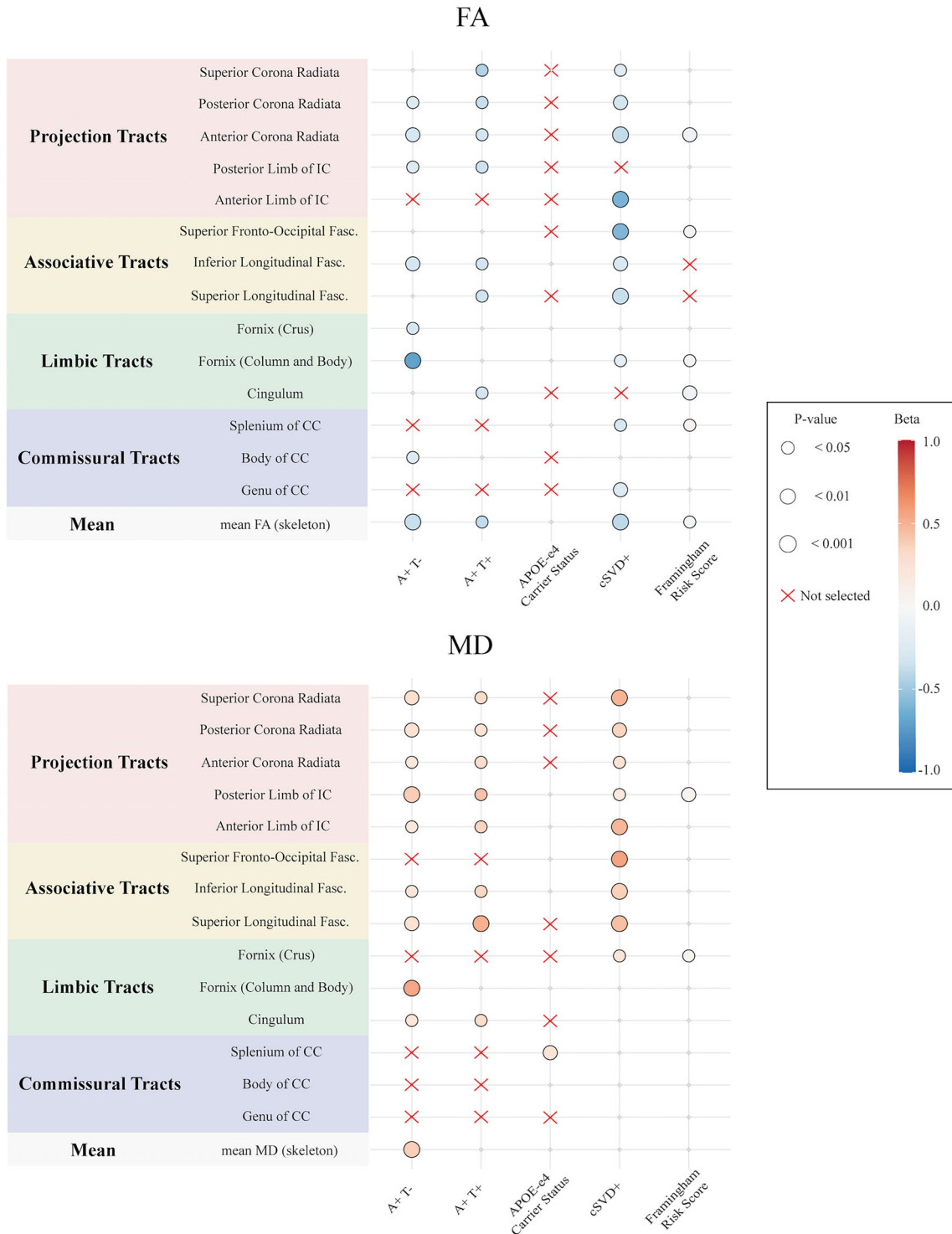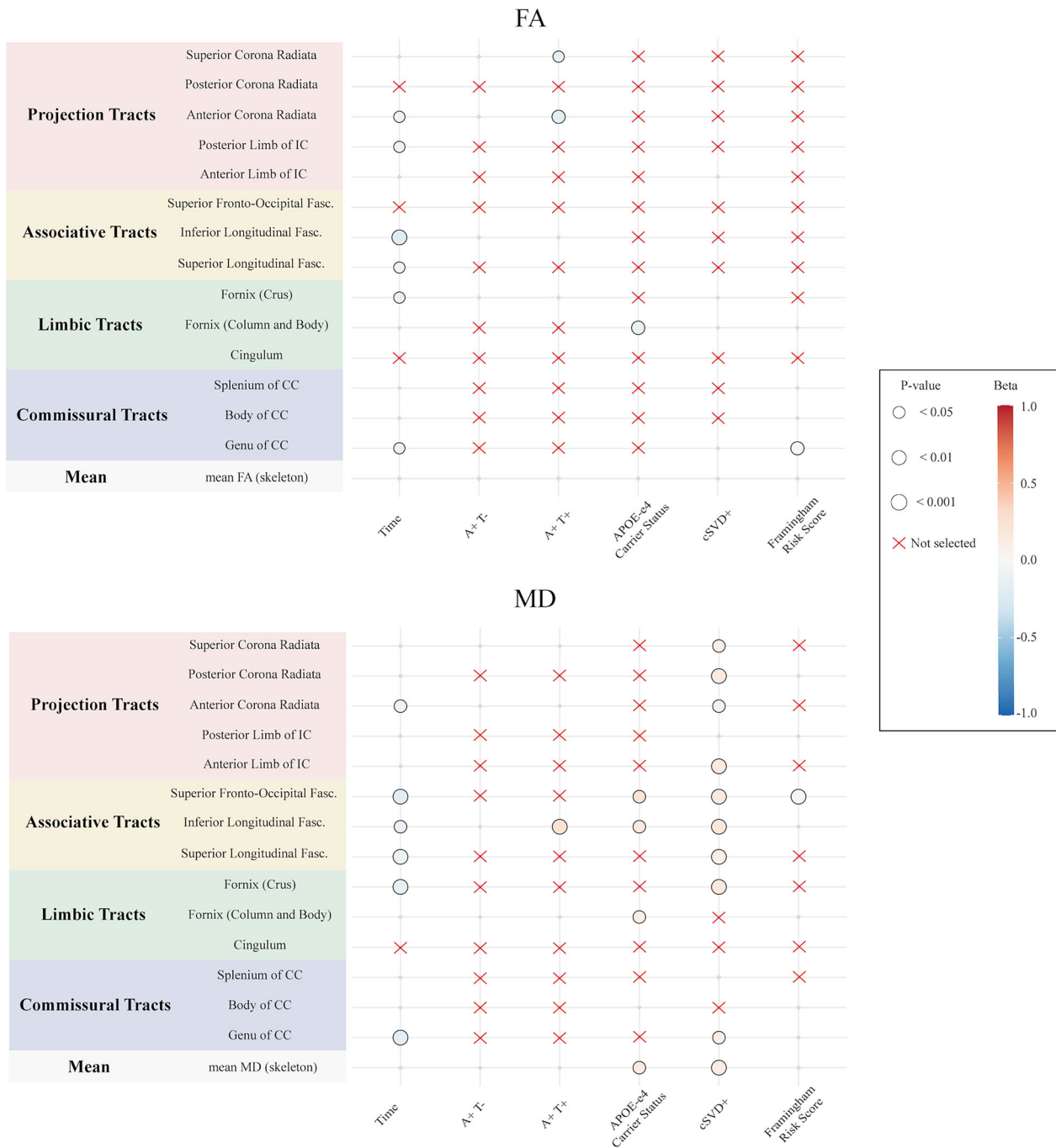# Determinants of WM cross-sectional integrity

Figure 3. Associations between WM cross-sectional integrity and AT status, APOE-ε4 carrier status, cSVD groups, and FRS. Heatmaps showing the significant associations ($p_{FDR} < 0.05$) between cross-sectional FA (upper section) or MD (bottom section) and linear mixed-effects models predictors. CC, corpus callosum; cSVD, cerebral small vessel disease; FA, fractional anisotropy; Fasc., fasciculus; FRS, Framingham risk score; IC, internal capsule; MD, mean diffusivity; WM, white matter.

Figure 4. Associations between WM longitudinal integrity and time, AT status, APOE-ε4 carrier status, cSVD groups, and FRS. Heatmaps showing the significant associations ($p_{FDR} < 0.05$) between longitudinal FA (upper section) or MD (bottom section) and linear mixed-effects models predictors. CC, corpus callosum; cSVD, cerebral small vessel disease; FA, fractional anisotropy; Fasc., fasciculus; FRS, Framingham risk score; IC, internal capsule; MD, mean diffusivity; WM, white matter.

At baseline, both A+T− and A+T+ participants showed significant lower FA and higher MD in most investigated projection tracts, except for the FA in the anterior limb of the internal capsule (all coefficients in Tables 2 and 3). A+T+ participants also had greater FA decline over time in the anterior ($\beta = -0.175$, $p = 0.01$) and superior

($\beta = -0.138$, $p = 0.01$) corona radiata. APOE-ε4 was not related to either baseline or longitudinal WM integrity in projection tracts.

At baseline, CSVD+ participants showed lower FA and higher MD in all investigated projections tract, except for FA in the posterior limb of the internal capsule (all coefficients in Tables 2 and 3). Similarly, greater increases of MD over time were observed in cSVD+ participants in all projection tracts but the posterior limb of the internal capsule (all coefficients in Table 3). Higher FRS scores were associated with lower FA in the anterior corona radiata ($\beta = -0.054$, $p = 0.001$) and higher MD in the posterior limb of the internal capsule ($\beta = 0.050$, $p = 0.008$).

Discussion

We investigated the effect of AD biomarkers, cSVD burden, and cardiovascular risk factors on WM microstructural integrity in non-demented older adults in the multi-center EPAD cohort. AD pathology ($A\beta_{1-42}$ and $p\text{-Tau}_{181}$) and APOE-ε4 had prominent effects on limbic tracts, while cSVD and FRS mostly impacted commissural, associative, and projection tracts. We showed that AD biomarkers and cSVD are independently associated with WM disruption in the explored tracts.

WM microstructural integrity of limbic tracts such as fornix (column body) and cingulum was found to be mostly impacted by AD biomarkers and APOE-ε4. This is in line with previous studies highlighting the involvement of these tracts, starting from AD preclinical stages,[27,28] as key structures of the Papez circuit, responsible for episodic memory functioning.[25] Indeed, diffusivity alterations of these tracts have been shown to predict tau accumulation in amyloid-positive individuals.[29] The strongest association was between A+T- status and fornix (column body) integrity, suggesting an early role of this structure. Similarly, decreases in fornix FA were previously shown to predict conversion from preserved cognition toward mild cognitive impairment and dementia,[27] further supporting its role in disease progression. The lack of association between A+T+ status and fornix microstructure could be due to the relatively low number of A+T+ participants. Nevertheless, evidence suggests a biphasic relationship between AD pathology and DTI scalars, as the inflammatory mechanisms linked to amyloid and tau accumulation (i.e., glial activation and cellular swelling) may cause changes opposing the typical neurodegeneration pattern.[1,30]

We observed widespread changes in white matter integrity in commissural, associative, and projection fibers, and demonstrated the presence of disease-specific gradients of WM disruption, anterior regions being more susceptible to vascular compromise and posterior regions to

AD-related factors. Specifically, WM integrity in the genu (anterior part) of CC was distinctively associated with cSVD+ and FRS, while both AD pathology and cSVD had a significant effect on body and splenium (middle and posterior parts). Moreover, while the posterior limb of the internal capsule was mainly impacted by AD-related factors, alterations of the anterior limb were more often observed in individuals with high cerebrovascular burden. This posterior–anterior gradient of WM deterioration is in line with the evidence of frontal WM being more sensitive to vascular health, and generally more susceptible to cerebrovascular insults.[31] Previous work has shown that global vascular health has a significant impact on white matter integrity, more strongly in the genu of the corpus callosum,[32] and several studies have shown the detrimental effect of single cardiovascular risk factors on commissural WM tracts, such as hypertension[33] and diabetes,[34] suggesting that this region is a proxy for cerebrovascular health.[32] Moreover, anterior patterns of WMHs have been shown to distinctively relate to cardiovascular etiologies.[35]

Conversely, WM lesions in parietal and occipital regions have been observed in association with amyloid pathology, independently of cardiovascular risk factors.[11] In line with our results, previous studies have shown amyloid pathology in relationship with alterations in a group of regions including medial, temporal, and posterior white matter.[36] The specific mechanisms through which amyloid deposition could impact white matter integrity are still unclear. On one hand, previous evidence has shown spatial correspondence between cortical amyloid deposition and white matter demyelination, possibly due to local alteration of neuronal and axonal function, thereby regulating oligodendrocyte functions, or resulting from Aβ-induced oxidative stress.[37] Conversely, Aβ deposition may enhance capillary cortical amyloid angiopathy (CAA) and arteriosclerosis,[38] resulting in hypoperfusion,[39] which may eventually lead to white matter damage through secondary vascular events.[37]

Given that AD pathology and cSVD often coexist from early stages of neurodegeneration,[40] questions have arisen regarding their impact on brain structure,[12,41,42] raising the need to determine whether they act separately or jointly in causing WM disruption.[15] Specifically, a recent *ex vivo* study has shown that the accumulation of WMHs is related to cSVD independently of AD pathology in non-demented older adults.[41] A fixel-based study has demonstrated that cSVD mainly impacts fiber density, while AD pathology has comparable effects on fiber density and cross-section,[42] leaving the question on their interaction unanswered. Here, we showed that they are both related to various degrees of disruption depending on the affected tracts, but seem to act largely

independently. Only APOE-ε4 (independently of Aβ$_{1-42}$ and p-Tau$_{181}$, both accounted for in the linear mixed-effects models)[43] showed interactions with FRS and cSVD+ in limbic and associative tracts. APOE-ε4 is involved in many amyloid-independent pathways affecting synaptic plasticity, metabolism, and vascular homeostasis,[44] and therefore possibly synergizing with other cSVD-specific inherited and acquired risk factors.[45] In this light, our results suggest that although sharing common etiopathological mechanisms, AD pathology and cSVD exert independent effects on white matter microstructure in preclinical stages. They also provide context for the selection of DTI metrics as outcome measures in primary and secondary prevention clinical trials, possibly representing a noninvasive alternative to PET imaging and a more sensitive MRI biomarker compared to hippocampal atrophy.[46] In particular, our findings indicate that limbic tracts would be most relevant for therapeutic strategies targeting the AT pathway, whereas commissural, associative, or projection tracts might be better choices for interventions targeting cerebrovascular mechanisms.

In line with previous evidence,[47] lower integrity measures were associated with higher age and male sex, with men showing higher MD in most of the tracts. In the posterior limb of the internal capsule, FA increased over time, possibly resulting from the relative sparing of the sensorimotor pathway in a crossing fibers region.[48] Similarly, in the anterior limb of internal capsule FA increased, due to the faster degradation of genu of CC fibers.[49] Some tracts showed a longitudinal MD decrease, supposedly due to the neuroinflammatory changes characterizing age-related neurodegeneration that may precede or overlap with microstructural disruption, causing temporary MD increases.[50] We were able to identify a greater number of significant longitudinal effects on MD compared to FA, supporting the evidence of MD being more sensitive than FA.[51]

Our study relies on a relatively large sample size and on the advantage of longitudinal data, but has also some limitations. Firstly, we used an atlas-based approach. As DTI tractography yields subject-specific masks and connectomes, further studies are warranted to confirm and expand our results. Using a simpler and robust approach, we showed that TBSS is sensitive to AD and cSVD associated factors. Considering its less demanding computational time and power compared to connectome analysis, TBSS application to large datasets and in the context of clinical trials is favored. Secondly, since our acquisition protocol comprised 30 diffusion directions only, we were limited to classical tensor-based analyses, with the limitation of being unable to resolve crossing fibers. Therefore, further studies are needed to confirm our findings, and possibly expand on them by exploring other DTI scalars, which we did not include to reduce the number of tests and increase our power to identify biological effects. Another limitation is the multicentric nature of the study, representing a confounding factor that could not be entirely removed using state-of-art harmonization methods. Nonetheless, this also implies the effects that we found must be robust as we were still able to observe them. Importantly, while our results provide information on the biological mechanisms underlying myelin disruption in healthy aging and disease, further studies are needed to translate our group findings to single subjects, which still represents one of the most demanding and still unsolved challenges of the entire field. While we decided to dichotomize Aβ1-42 and p-Tau181 to adhere to the biological definition of AD and to the ATN framework, and subsequently we used gaussian mixture modeling to identify a cut-off to dichotomize cSVD and make it comparable to the ATN classification, further studies could explore the relationship between WM integrity and continuous measure of amyloid and tau accumulation or cSVD burden. Lastly, further research is needed to model the nonlinear relationship between amyloid and WM integrity.[1,30]

In conclusion, we showed that AD pathology and cSVD are independently associated with myelin microstructural integrity within several tracts, with pathology-specific spatial patterns of WM vulnerability. This evidence supports the role of DTI for disease monitoring and subjects selection for early intervention targeting the factors associated with increased risk of developing dementia.

Acknowledgements

Author Contributions

M.T, L.L., and F.B. contributed to the conception and design of the study and to drafting the manuscript; M.T, L.L., L.E.C., D.V.G., and F.B. contributed to the acquisition and analysis of the data and interpretation of the results; M.T, L.L., L.E.C., D.V.G., S.I., G.P., L.P., A.M., R.W., S.H., K.B., G.F., C.H.S., G.C., M.E., P.P., A.W.,

References

1. Pichet Binette A, Theaud G, Rheault F, et al. Bundle-specific associations between white matter microstructure and Aβ and tau pathology in preclinical Alzheimer's disease [Internet]. elife. 2021;10:e62929. doi:10.7554/eLife.62929

2. Tuladhar AM, van Norden AGW, de Laat KF, et al. White matter integrity in small vessel disease is related to cognition. Neuroimage Clin. 2015;7:518-524.

3. Cuadrado-Godia E, Dwivedi P, Sharma S, et al. Cerebral small vessel disease: a review focusing on pathophysiology, biomarkers, and machine learning strategies. J Stroke Cerebrovasc Dis. 2018;20(3):302-320.

4. Desai MK, Mastrangelo MA, Ryan DA, Sudol KL, Narrow WC, Bowers WJ. Early oligodendrocyte/myelin pathology in Alzheimer's disease mice constitutes a novel therapeutic target. Am J Pathol. 2010;177(3):1422-1435.

5. Chao LL, Decarli C, Kriger S, et al. Associations between white matter hyperintensities and β amyloid on integrity of projection, association, and limbic fiber tracts measured with diffusion tensor MRI. PLoS One. 2013;8(6):e65175.

6. Akoudad S, de Groot M, Koudstaal PJ, et al. Cerebral microbleeds are related to loss of white matter structural integrity. Neurology. 2013;81(22):1930-1937.

7. Freeze WM, Jacobs HIL, Gronenschild EH, et al. White matter Hyperintensities potentiate hippocampal volume reduction in non-demented older individuals with abnormal amyloid-β. J Alzheimers Dis. 2017;55(1):333-342.

8. Shirzadi Z, Schultz SA, Yau W-YW, et al. Etiology of white matter hyperintensities in autosomal dominant and sporadic Alzheimer disease [Internet]. JAMA Neurol. 2023;80:1353-1363. doi:10.1001/jamaneurol.2023.3618

9. Storsve AB, Fjell AM, Yendiki A, Walhovd KB. Longitudinal changes in white matter tract integrity across the adult lifespan and its relation to cortical thinning. PLoS One. 2016;11(6):e0156770.

10. Assaf Y, Pasternak O. Diffusion tensor imaging (DTI)-based white matter mapping in brain research: a review. J Mol Neurosci. 2008;34(1):51-61.

11. Pålhaugen L, Sudre CH, Tecelao S, et al. Brain amyloid and vascular risk are related to distinct white matter hyperintensity patterns. J Cereb Blood Flow Metab. 2020;41:1162-1174.

12. Vemuri P, Lesnick TG, Knopman DS, et al. Amyloid, vascular, and resilience pathways associated with cognitive aging. Ann Neurol. 2019;86(6):866-877.

13. Aisen PS, Jimenez-Maggiora GA, Rafii MS, Walter S, Raman R. Early-stage Alzheimer disease: getting trial-ready. Nat Rev Neurol. 2022;18(7):389-399.

14. Wardlaw JM, Woodhouse LJ, Mhlanga II, et al. Isosorbide mononitrate and cilostazol treatment in patients with symptomatic cerebral small vessel disease: the lacunar intervention Trial-2 (LACI-2) randomized clinical trial. JAMA Neurol. 2023;80(7):682-692.

15. Koops EA, Jacobs HIL. Untangling white matter fibre changes in Alzheimer's disease and small vessel disease. Brain. 2023;146(2):413-415.

16. Ngandu T, Lehtisalo J, Solomon A, et al. A 2 year multidomain intervention of diet, exercise, cognitive training, and vascular risk monitoring versus control to prevent cognitive decline in at-risk elderly people (FINGER): a randomised controlled trial. Lancet. 2015;385 (9984):2255-2263.

17. Solomon A, Kivipelto M, Molinuevo JL, Tom B, Ritchie CW, EPAD Consortium. European prevention of Alzheimer's dementia longitudinal cohort study (EPAD LCS): study protocol. BMJ Open. 2019;8(12):e021017.

18. Ingala S, De Boer C, Masselink LA, et al. Application of the ATN classification scheme in a population without dementia: findings from the EPAD cohort [Internet]. Alzheimers Dement. 2021;17:1189-1204. doi:10.1002/alz. 12292

19. Wardlaw JM, Smith EE, Biessels GJ, et al. Neuroimaging standards for research into small vessel disease and its contribution to ageing and neurodegeneration [Internet]. Lancet Neurol. 2013;12(8):822-838. doi:10.1016/s1474-4422(13)70124-8

20. D'Agostino RB Sr, Vasan RS, Pencina MJ, et al. General cardiovascular risk profile for use in primary care: the Framingham heart study. Circulation. 2008;117 (6):743-753.

21. Calvin CM, de Boer C, Raymont V, et al. Continuous and risk-score-based predictors of ATN Alzheimer's disease status among cognitively healthy individuals: findings from the EPAD-LCS study [Internet]. Alzheimers Dement. 2020;16(S5):e041097. doi:10.1002/alz.041097

22. Lorenzini L, Ingala S, Wink AM, et al. The European prevention of Alzheimer's dementia (EPAD) MRI dataset and processing workflow [Internet]. bioRxiv 2021. doi:10.1101/2021.09.29.462349.abstract

23. Smith SM, Jenkinson M, Johansen-Berg H, et al. Tract-based spatial statistics: voxelwise analysis of multi-subject diffusion data. NeuroImage. 2006;31 (4):1487-1505.

24. Wakana S, Jiang H, Nagae-Poetscher LM, van Zijl PCM, Mori S. Fiber tract–based atlas of human white matter anatomy. Radiology. 2004;230(1):77-87.

25. Aggleton JP, Nelson AJD, O'Mara SM. Time to retire the serial Papez circuit: implications for space, memory, and attention. Neurosci Biobehav Rev. 2022;140:104813.

26. Fortin J-P, Cullen N, Sheline YI, et al. Harmonization of cortical thickness measurements across scanners and sites. NeuroImage. 2018;167:104-120.

27. Oishi K, Lyketsos CG. Alzheimer's disease and the fornix. Front Aging Neurosci. 2014;6:241.

28. Alm KH, Bakker A. Relationships between diffusion tensor imaging and cerebrospinal fluid metrics in early stages of the Alzheimer's disease continuum. J Alzheimers Dis. 2019;70(4):965-981.

29. Jacobs HIL, Hedden T, Schultz AP, et al. Structural tract alterations predict downstream tau accumulation in amyloid-positive older individuals. Nat Neurosci. 2018;21 (3):424-431.

30. Collij LE, Ingala S, Top H, et al. White matter microstructure disruption in early stage amyloid pathology. Alzheimers Dement. 2021;13(1):e12124.

31. Lamar M, Boots EA, Arfanakis K, Barnes LL, Schneider JA. Common brain structural alterations associated with cardiovascular disease risk factors and Alzheimer's dementia: future directions and implications. Neuropsychol Rev. 2020;30(4):546-557.

32. Vemuri P, Lesnick TG, Przybelski SA, et al. Development of a cerebrovascular magnetic resonance imaging biomarker for cognitive aging. Ann Neurol. 2018;84(5):705-716.

33. Gons RAR, van Oudheusden LJB, de Laat KF, et al. Hypertension is related to the microstructure of the corpus callosum: the RUN DMC study. J Alzheimers Dis. 2012;32(3):623-631.

34. Tan X, Fang P, An J, et al. Micro-structural white matter abnormalities in type 2 diabetic patients: a DTI study using TBSS analysis. Neuroradiology. 2016;58(12):1209-1216.

35. Lorenzini L, Ansems LT, Lopes Alves I, et al. Regional associations of white matter hyperintensities and early cortical amyloid pathology. Brain Commun. 2022;4(3): fcac150.

36. Acosta-Cabronero J, Alley S, Williams GB, Pengas G, Nestor PJ. Diffusion tensor metrics as biomarkers in Alzheimer's disease. PLoS One. 2012;7(11):e49072.

37. Caballero MÁA, Song Z, Rubinski A, et al. Age-dependent amyloid deposition is associated with white matter alterations in cognitively normal adults during the adult life span. Alzheimers Dement. 2020;16(4):651-661.

38. Weller RO, Boche D, Nicoll JAR. Microvasculature changes and cerebral amyloid angiopathy in Alzheimer's disease and their potential impact on therapy. Acta Neuropathol. 2009;118(1):87-102.

39. Kisler K, Nelson AR, Montagne A, Zlokovic BV. Cerebral blood flow regulation and neurovascular dysfunction in Alzheimer disease. Nat Rev Neurosci. 2017;18(7):419-434.

40. Schneider JA, Arvanitakis Z, Bang W, Bennett DA. Mixed brain pathologies account for most dementia cases in community-dwelling older persons. Neurology. 2007;69 (24):2197-2204.

41. Arfanakis K, Evia AM, Leurgans SE, et al. Neuropathologic correlates of white matter hyperintensities in a community-based cohort of older adults. J Alzheimers Dis. 2020;73(1):333-345.

42. Dewenter A, Jacob MA, Cai M, et al. Disentangling the effects of Alzheimer's and small vessel disease on white matter fibre tracts. Brain. 2023;146(2):678-689.

43. Yamazaki Y, Zhao N, Caulfield TR, Liu CC, Bu G. Apolipoprotein E and Alzheimer disease: pathobiology and targeting strategies. Nat Rev Neurol. 2019;15(9):501-518.

44. Liao F, Yoon H, Kim J. Apolipoprotein E metabolism and functions in brain and its role in Alzheimer's disease. Curr Opin Lipidol. 2017;28(1):60-67.

45. Inoue Y, Shue F, Bu G, Kanekiyo T. Pathophysiology and probable etiology of cerebral small vessel disease in vascular dementia and Alzheimer's disease. Mol Neurodegener. 2023;18(1):46.

46. Falgàs N, Sánchez-Valle R, Bargalló N, et al. Hippocampal atrophy has limited usefulness as a diagnostic biomarker on the early onset Alzheimer's disease patients: a comparison between visual and quantitative assessment. Neuroimage Clin. 2019;23:101927.

47. Lawrence KE, Nabulsi L, Santhalingam V, et al. Age and sex effects on advanced white matter microstructure measures in 15,628 older adults: a UK Biobank Study. Brain Imaging Behav. 2021;15(6):2813-2823.

48. de Groot M, Cremers LGM, Ikram MA, et al. White matter degeneration with aging: longitudinal diffusion MR imaging analysis. Radiology. 2016;279(2):532-541.

49. Wiegell MR, Larsson HB, Wedeen VJ. Fiber crossing in human brain depicted with diffusion tensor MR imaging. Radiology. 2000;217(3):897-903.

50. Finger CE, Moreno-Gonzalez I, Gutierrez A, Moruno-Manchon JF, McCullough LD. Age-related immune alterations and cerebrovascular inflammation. Mol Psychiatry. 2022;27(2):803-818.

51. Luque Laguna PA, Combes AJE, Streffer J, et al. Reproducibility, reliability and variability of FA and MD in the older healthy population: a test-retest multiparametric analysis. Neuroimage Clin. 2020;26:102168.

Supporting Information

Additional supporting information may be found online in the Supporting Information section at the end of the article.

Data S1 Supporting Information.